

2
①
NRL Report 6869

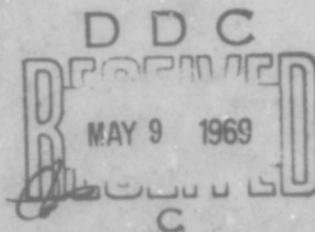
AD 686661

Dislocation Pipe Diffusion in Silver Single Crystals

R. G. VARDIMAN AND M. R. ACHTER

*Thermostructural Materials Branch
Metallurgy Division*

March 25, 1969



NAVAL RESEARCH LABORATORY
Washington, D.C.

This document has been approved for public release and sale; its distribution is unlimited.

Reproduced by the
CLEARINGHOUSE
for Federal Scientific & Technical
Information Springfield Va. 22151

14

CONTENTS

Abstract	ii
Problem Status	ii
Authorization	ii
INTRODUCTION	1
EXPERIMENTAL METHODS	1
General Technique	1
Specimen Preparation	1
Diffusion, Sectioning, and Counting	2
Calculation of D	3
RESULTS	6
DISCUSSION	7
ACKNOWLEDGMENTS	8
REFERENCES	9

ABSTRACT

A chemical sectioning technique has been developed for the measurement of self diffusion in silver at low temperatures. (Silver was chosen because of its well-established high-temperature behavior, and because of the availability of the long-lived isotope Ag^{110} .) Layers of 100A or less are removed by an iodine reaction, and diffusion coefficients D as low as 2×10^{-17} cm^2/sec have been measured. A large enhancement over extrapolated high-temperature values, which has been observed below $T_m/2$, is attributed to dislocation short circuiting. Determination of the pipe diffusion coefficient at the lowest measured temperature, where Harrison's type C kinetics are expected to apply, yields good agreement with the pipe diffusion coefficients D_p calculated from published data obtained by another technique.

PROBLEM STATUS

This report completes one phase of the problem; work is continuing on other phases of the problem.

AUTHORIZATION

NRL Problem M01-09
Project RR 007-01-46-5407

Manuscript submitted December 6, 1968.

DISLOCATION PIPE DIFFUSION IN SILVER SINGLE CRYSTALS

INTRODUCTION

Measurements of diffusion coefficients at temperatures below those where the usual techniques have been applied are of considerable interest. Such measurements are useful, for example, in the study of radiation-enhanced diffusion, strain-enhanced diffusion, and dislocation pipe diffusion, as well as for determining the applicability of the Arrhenius equation over greater temperature ranges.

In the past, only unusual techniques of limited applicability, such as the atomic recoil method in α -particle emitters (1) or the counting of low-energy β 's in nickel (2), could measure directly diffusion coefficient values less than 10^{-14} cm²/sec. Recently an anodizing technique (3) has been applied to niobium and tantalum (4,5) with coefficient values D measured in the 10^{-18} cm²/sec range.

Silver was chosen for the present study because of its well-established high-temperature behavior and because of the availability of the long-lived isotope Ag¹¹⁰. The value of $D = 0.40 \exp(-44,090/RT)$ found by Tomizuka and Sonder (6) is taken here as the best available.

A summary of the experimental technique, along with a discussion of the results, has been published in Trans. AIME (7).

EXPERIMENTAL METHODS

General Technique

A modification of the surface tracer technique was developed for the present study, employing a chemical sectioning method for the determination of diffusion-penetration curves. Silver single crystals were electroplated with the isotope Ag¹¹⁰ and diffused at a series of temperatures. Sectioning was accomplished by reacting the surface with iodine and removing the resultant thin AgI layer with a cyanide solution, whose activity was then used for the calculation of D .

Specimen Preparation

Because of the extremely small penetration distances involved, great care had to be taken in specimen preparation. Silver single crystals of 99.995% purity, grown from the melt as 3/4-in. rods, were obtained from Semi-Elements, Inc. It was found that a strain-free surface, as indicated by back-reflection x rays, could be obtained by cutting 1/8-in. discs in an abrasive cutoff wheel, hand polishing through 3/0 paper, and removing approximately 0.004 in. by electropolishing.

Of the number of electropolishing solutions tried, the most satisfactory contained 90 g/l KCN, 30 g/l AgCN, and 30 g/l K₂CO₃. An initial conditioning was required, which involved polishing for 1 to 2 amp-hr under normal polishing conditions. The same solution was used for all experiments, with occasional additions of KCN to restore optimum

polishing conditions. A 1000-ml beaker containing 500 ml of electrolyte, with a stainless steel cathode on one side and a glass stirrer inserted from the top, was used. It was found necessary to place the polishing bath in an ultrasonic vibrator to eliminate roughness, apparently due to microscopic bubbles which clung to the surface of the specimen. The silver specimen was encased in a wax mold to confine polishing and plating to one face, with electrical contact provided by a stainless steel strip through the side of the mold.

Polishing characteristics, which varied according to solution composition, age, and other characteristics, generally adhered to the following pattern: At low voltages etching occurred, and when the voltage was raised to about 1.5 V large and rapid fluctuations of current were observed. Above 2 V polishing took place, with formation of a viscous film on the specimen surface which increased in density with increasing voltage. The voltage and stirring had to be adjusted so that the film did not stick to and build up on the surface of the specimen. It was also necessary to balance the stirring rate against the action of the ultrasonic vibrator to avoid serious surface distortions. Best results were obtained by polishing at 3 to 4 V, then dropping the voltage to 2 V or less for a few seconds before the specimen was removed from the bath. The final voltage drop was necessary to eliminate any film which might remain on the specimen surface, as such areas were generally microscopically rough. Current density varied with bath age and composition, but generally ranged from 100 to 150 mA/cm². Usually, the above procedure produced a bright, microscopically smooth surface, with few artifacts. A slight macroscopic waviness was observed, however, due to the ultrasonic, but this was not considered a problem.

Electrodeposition was achieved by a standard plating bath which contained 53 g/l KCN, 37 g/l AgCN, and 40 g/l K₂CO₃. To 500 ml of this solution in a 1000-ml beaker was added 3 mCi of Ag¹¹⁰, in the form of AgNO₃, obtained from the Isotope Division, Oak Ridge National Laboratory. A silver anode of approximately 0.5 cm² area was used. Best results were obtained at 0.1 V and a current density of 1 mA/cm², with mild stirring. In order to prevent mottling and unevenness in the deposit, precautions were taken to keep the specimen surface clean. After electropolishing, the specimen was made the cathode in a detergent solution and cleaned by hydrogen bubbling at 10 V. The surface was then pickled in dilute HCl. After washing in distilled water, a covering of water was left on the surface as the specimen was inserted horizontally into the plating bath. This procedure gave a clear, even plating, which should be coherent and essentially strain free (8). Measurement of the plating thickness, which was generally 500 to 1000 Å, is described under "Calculation of *D*."

For determination of the dislocation density, one crystal was sectioned on the {111} plane by spark cutting. After polishing through 3/0 paper, the chemical polishing and etch pitting technique of Levinstein and Robinson (9) was used to develop pits at dislocation sites.

Diffusion, Sectioning, and Counting

An air-circulating muffle furnace was used for the diffusion anneals. Temperature control was, on the average, to within ±1°C. Below 400°C oxidation reactions made it necessary to place the specimen in an evacuated Pyrex capsule. Diffusion anneals were made at 448, 373, 338, and 258°C (see Table 1). No loss of radioactive material was detected at any temperature.

Sectioning was performed in two steps. After masking the outer edge of the sample, leaving an area of about 2 cm² (slightly smaller than the original plating), the surface was immersed in a solution of 0.5 g/l of iodine in alcohol for 1 to 1-1/2 min depending

Table 1
Measurements Associated with the Electroplating, Diffusion Annealing,
and Sectioning of Silver Single Crystals in order to Obtain Values for
the Diffusion Coefficient

Spec.	Plating Thickness (Å)	Diff. Anneal Temp. (°C)	Diff. Anneal Time (sec)	Stripped Layer Thickness (Å)	$\frac{\sqrt{Dt}}{h}$	Diff. Coeff. D (cm ² /sec)
C	973	448	3.60×10^3	84	0.97	2.47×10^{-14}
F	953	373	1.275×10^5	84	1.16	9.6×10^{-16}
G	956	338	1.03×10^6	100	1.72	2.64×10^{-16}
H	460	258	2.75×10^6	66	1.59	1.94×10^{-17}

on the solution reaction rate. A very even layer of AgI was formed, which was insoluble in water or alcohol. In the second step the specimen was immersed with agitation in a beaker which contained 20 cc of a solution of 1.0 g/l KCN in water. The iodide dissolved in a few seconds while the silver below was attacked only very slowly. The cyanide solution was then evaporated to a small volume and transferred to a vial for counting. Ten to fifteen layers were removed per specimen.

The reaction rate of the iodine solution varied slightly over a period of time, so that the thickness of the stripped layers, while quite regular for a given specimen, ranged from 65 to 100Å for different specimens, as described under "Calculation of D ." The dissolution took place quite evenly; interferometric measurements at the masked edge of a completely stripped sample showed a reasonably even, single step of the correct size.

Counting was carried out in a well-type scintillation counter with a single-channel radiation analyzer and scaler. The complex spectrum of Ag¹¹⁰ precludes counting a specific energy, so the analyzer was set to accept all energies above 90 kV. It was determined that no betas were being counted. For counting the plated specimen, a special holder was made so that it sat just above the crystal well, a configuration which gave reproducible geometry. Appropriate decay corrections were made on all counts.

Calculation of D

Because of the small penetration distances, it is necessary to use the exact solution of Fick's law for a source of finite thickness (10). For a plating of thickness h ,

$$C/C_0 = 1/2 \left[\operatorname{erf} \left(\frac{1 - (x/h)}{2\sqrt{Dt}/h} \right) + \operatorname{erf} \left(\frac{1 + (x/h)}{2\sqrt{Dt}/h} \right) \right] \quad (1)$$

where C is the concentration at depth x , erf is the error function, D is the apparent diffusion coefficient, and t is the time.

For the boundary conditions used in this experiment, it is necessary to know the average plating thickness accurately. The 1000Å plates used in diffusion were too thin for accurate weighing, so plates of 2500 to 10,000Å thickness were prepared, with the plating area exactly defined by masking the outer edge prior to deposition. The weight gain was determined on a semimicro balance, and a plot of plating weight vs γ -ray activity for the series of specimens, as in Fig. 1, allowed the thickness of any plating to be

The ratio of the length to the radius of the elements is fixed at 1000. The technique described in Ref. 1 is used to calculate the load currents.

We calculate h_{ei} and Z_{ai} from a load impedance pair A and again for a load impedance pair B . The load impedance pairs used in this example are

$$Z_{\ell} - \text{Pair } A = \begin{bmatrix} 60 - jX \\ 240 + jX \end{bmatrix}$$

and

$$Z_{\ell} - \text{Pair } B = \begin{bmatrix} 60 + jX \\ 240 - jX \end{bmatrix}$$

where $X = 1150 - 740 \beta_0 h$ (note that $X = 0$ at approximately $\beta_0 h = \pi/2$ where an isolated element resonates).

Our final results, which we present in the figures to follow, are the arithmetic average of the values of h_{ei} and Z_{ai} obtained from the two load impedance pairs A and B .

RESULTS

In Fig. 3 we present the resistance and reactance of the first element of the array as functions of the angle of incidence of the illumination with the electrical half length of the elements $\beta_0 h$ held fixed at various values.

We observe from Fig. 3 that the resistance and reactance vary rather slowly with ϕ_{inc} for values of $\beta_0 h$ of $\pi/2$ or less. For values of $\beta_0 h$ of 1.8 or more the resistance varies rapidly at the higher angles of incidence. The reactance changes quite a bit in this region also but not as rapidly as the resistance. Figure 3 also shows the real part (h_e/h) and the imaginary part (h_e''/h) of the relative effective length (h_e/h) of the first element plotted in like manner. It is apparent that the real part of h_e/h remains a relatively slowly varying function of ϕ_{inc} even at the higher values of $\beta_0 h$. The imaginary part of h_e/h for $\beta_0 h = 2$ appears to change considerably with ϕ_{inc} ; but for the lower values of $\beta_0 h$ the imaginary part of h_e/h remains rather small in value and almost invariant with ϕ_{inc} .

In Figs. 4, 5, and 6, we present the calculated impedance and effective length information for elements 3, 5, and 8, respectively. Because of mutual coupling effects the results for the various elements of the array differ in certain respects.

In Table 1 we present a comparison of the load currents calculated from Eq. (4) with the load currents arrived at by the more lengthy method of Ref. 1. The comparison is made for several load impedances, none of which is a member of the reference pair of load impedances used in determining the h_e and Z_a of the elements.

An examination of Table 1 shows that the largest phase difference (-2.94 degrees) occurs in the first element and that the current ratio deviates from unity by the largest amount (6.5 percent) in element 7, both taken from Table 1a, where $\beta_0 h = 1.57$ and the load impedance is (480 - j480) ohms.

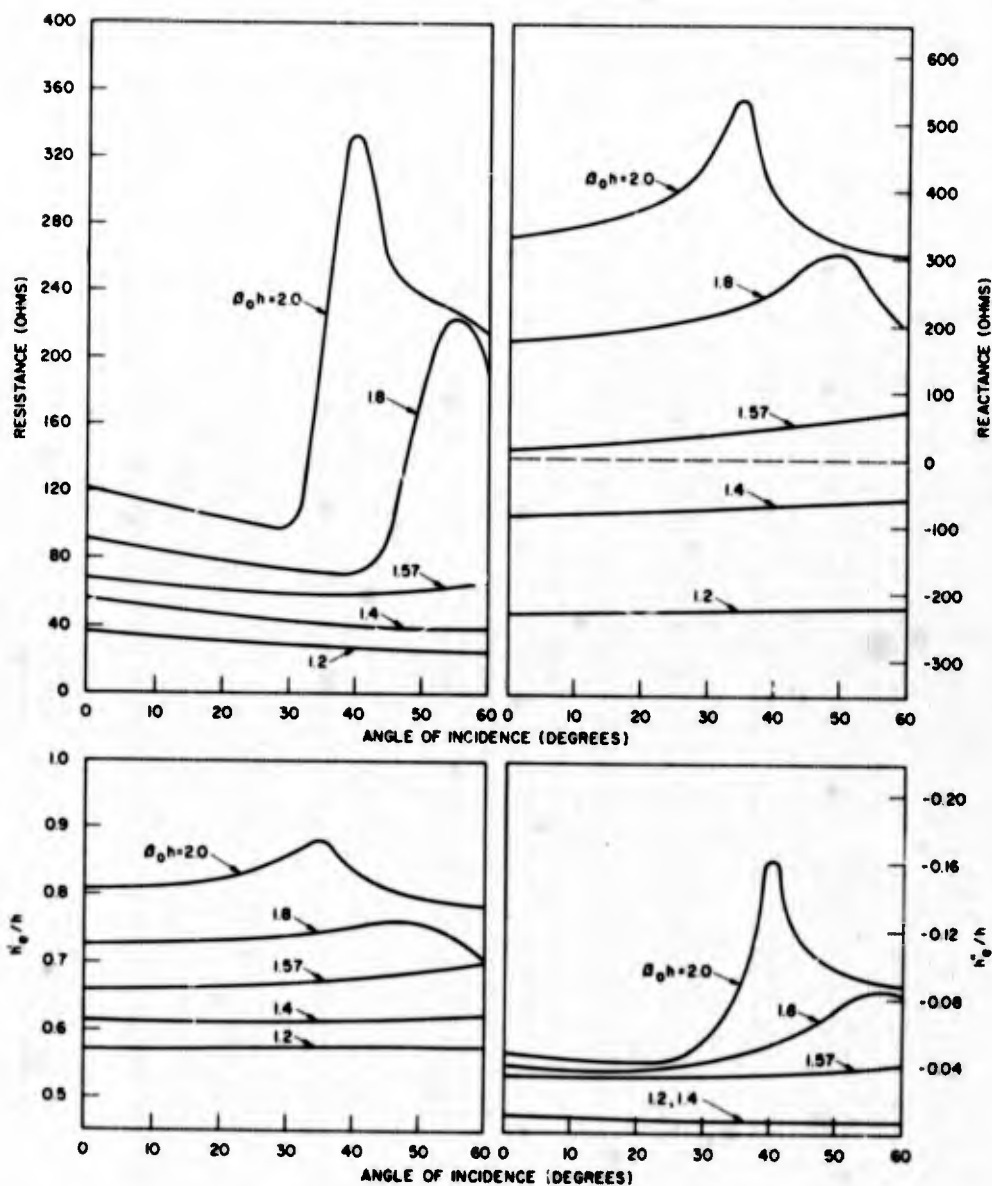


Fig. 3 - The internal impedance and effective half-length of the first element as a function of angle of incidence. The upper left gives the internal resistance; the upper right, the internal reactance; the lower left, the real part of h_e/h ; and the lower right, the imaginary part of h_e/h .

The diffusion coefficient D may be obtained from the concentration-penetration data in two ways. In the first method, C/C_0 is plotted versus x/h , and D is found by fitting the data to Eq. (1) for the best value of \sqrt{Dt}/h . In the alternative method, which was used for this work, the value of the concentration was determined at $x = 0$, where

$$C/C_0 = \text{erf}(h^2 \sqrt{Dt}) .$$

Enough points were taken to impart confidence in the accuracy of the intersection.

At each temperature of diffusion, the time t was estimated to give values of \sqrt{Dt}/h between 1.0 and 1.7. A high value is desirable to minimize the error introduced by the apparent diffusion in the as-plated specimen, as in Fig. 2(a). On the other hand, too high a value leads to loss of sensitivity because of the flatness of the diffusion penetration curve.

RESULTS

A typical concentration-penetration curve is given in Fig. 3. No sharp changes are observed in crossing from the original plating depth to the initially unplated material.

Data for the four temperatures used in the present investigation are given in Table 1, and the experimental diffusion coefficients are plotted in Fig. 4, along with the extrapolation of the high-temperature data of Tomizuka and Sonder (6). In order to keep the parameter \sqrt{Dt}/h within the desired limits, 450°C is the highest feasible temperature with a 1000Å plate, and a diffusion time of at least 1 hr. Likewise, at 250°C parametric and time limitations required a reduction of plating thickness to 500Å.

Dislocation densities obtained from etch pit counts averaged $5 \times 10^7 \text{ cm}^{-2}$, comparable to the values of $1-5 \times 10^7$ found by Levinstein and Robinson (9) in annealed melt-grown single crystals. The density was fairly uniform, with scarcely any substructure.

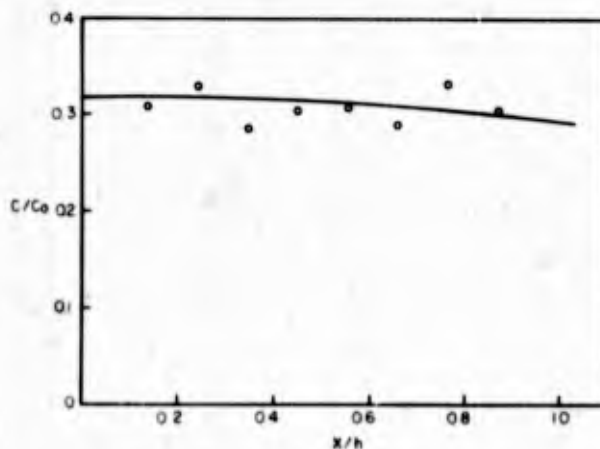


Fig. 3 - Example of a concentration-penetration curve

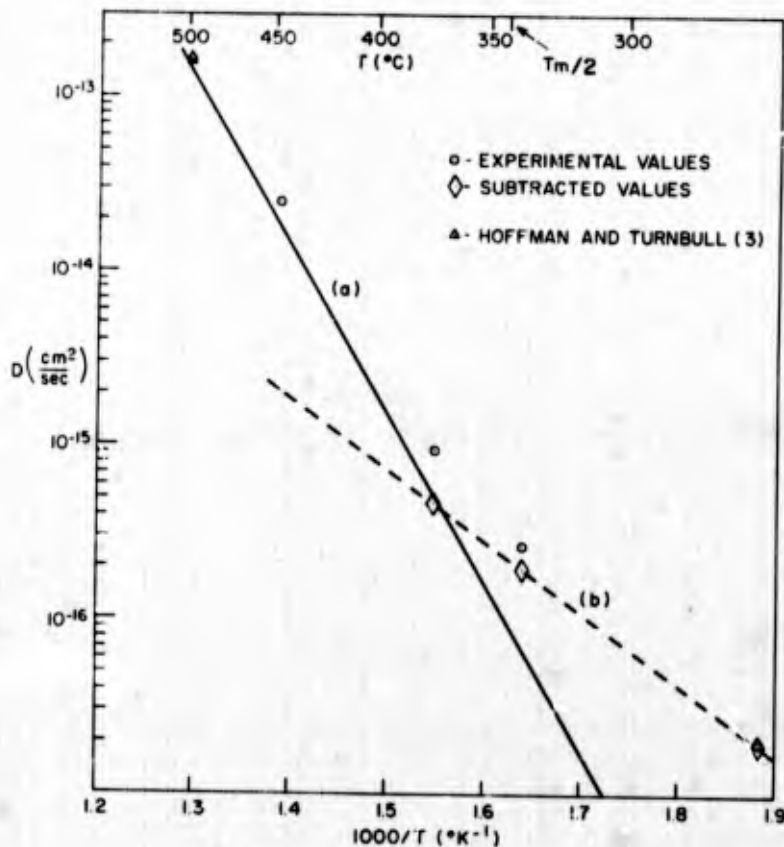


Fig. 4 - Temperature dependence of diffusion coefficients D showing experimental values and derived curves. Curve (a) shows extrapolation of high-temperature data (6); curve (b) is the difference between curve (a) and experimental values.

DISCUSSION

The diffusion coefficient at the highest measured temperature (448°C) agrees reasonably well with the extrapolation from high-temperature data. The lower temperature points deviate strongly from the extrapolation. The data can be fitted by two straight lines on the semilog plot: the high-temperature equation $D = 0.40 \exp(-44,090/RT)$, plus the equation $D' = 1.0 \times 10^{-9} \exp(-18,800/RT)$. The points on the D' curve (Fig. 4(b)) were obtained by subtraction of the extrapolated high-temperature D values from the experimental D values.

The enhancement of low-temperature diffusion is of a degree to suggest short circuiting by dislocations. This is supported by the activation energy for D' of 18,800 cal/mole, which is in good agreement with the value 19,700 cal/mole given by Turnbull and Hoffman (11) for diffusion in low-angle boundaries in silver.

The value of D' at 450°C is small compared to the high-temperature or lattice diffusion value, so enhancement at this temperature would be difficult to observe. The two lowest data points of Hoffman and Turnbull (12) at 500°C are included in Fig. 4 and are seen to agree well with curve (a), showing no enhancement. Hart (13) analyzed simultaneous lattice and pipe diffusion and showed that some enhancement might be expected at 500°C. However, his calculations imply a value of ten atoms "in" a dislocation on a plane perpendicular to it (14), while according to Love (15) the dislocation diffusion pipe consists only of the row of sites at the core of the dislocation, one-tenth of the above value.

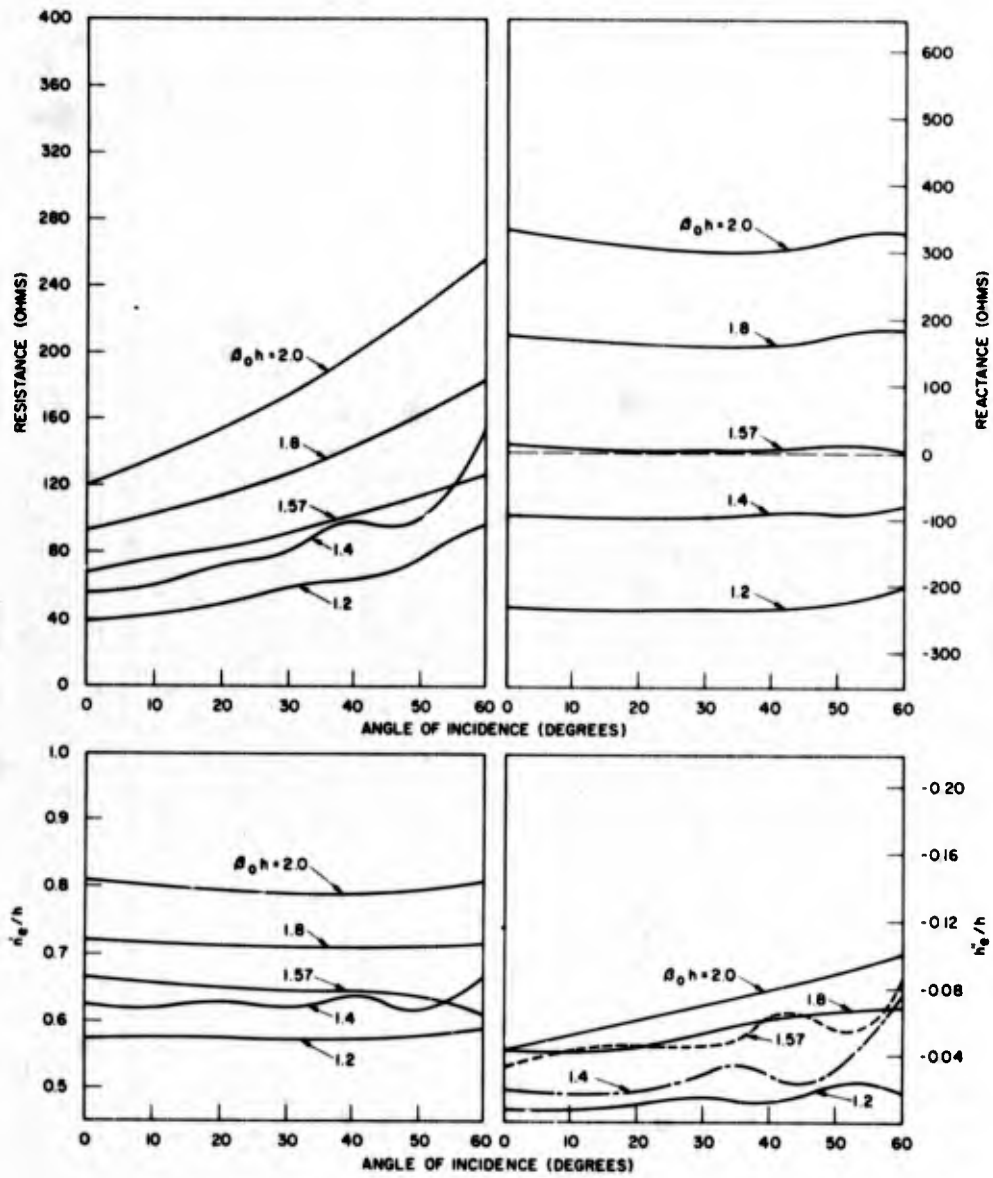


Fig. 6 - The internal impedance and effective half-length of the eighth element as a function of angle of incidence. The upper left gives the internal resistance; the upper right, the internal reactance; the lower left, the real part of h_e/h ; and the lower right, the imaginary part of h_e/h .

Table 1a - Comparison of Load Currents From Eq. (4) With Those From the Method of Ref. 1 for $\beta_{0h} = 1.57$ and Load Impedances 480 - j480 ohms

Element Number	Current Ratio	Phase Difference (degrees)
$\phi_{inc} = 0$ degree		
1	0.994	-0.43
2	1.008	0.44
3	0.995	-0.22
4	1.001	0.06
5	1.001	0.06
6	0.995	-0.22
7	1.008	0.44
8	0.994	-0.43
$\phi_{inc} = -20$ degrees		
1	0.993	-1.03
2	0.978	0.98
3	1.021	0.27
4	0.995	-1.10
5	0.984	0.74
6	1.018	0.50
7	1.003	-1.23
8	0.981	-0.09
$\phi_{inc} = -40$ degrees		
1	0.991	-1.41
2	0.982	-0.91
3	0.979	1.06
4	1.014	1.32
5	1.025	-0.32
6	1.006	-1.44
7	1.030	-1.17
8	0.968	-0.36
$\phi_{inc} = -60$ degrees		
1	0.993	-2.94
2	0.996	-1.28
3	0.997	1.29
4	0.988	-1.59
5	0.971	-1.48
6	0.955	-0.74
7	0.945	0.43
8	0.936	1.02

Table 1b - Comparison of Load Currents From Eq. (4) With Those From the Method of Ref. 1 for $\beta_{0h} = 1.57$ and Load Impedances 120 - j120 ohms

Element Number	Current Ratio	Phase Difference (degrees)
$\phi_{inc} = -40$ degrees		
1	0.991	0.81
2	0.999	0.69
3	1.015	0.01
4	1.001	-0.88
5	0.986	-0.37
6	0.987	0.50
7	0.999	1.04
8	1.008	0.92
$\phi_{inc} = -60$ degrees		
1	0.981	1.52
2	0.997	1.51
3	0.994	0.46
4	0.995	0.91
5	1.004	1.30
6	1.018	1.31
7	1.031	0.95
8	1.032	0.80

Table 1c - Comparison of Load Currents From Eq. (4) With Those From the Method of Ref. 1 for $\beta_{0h} = 1.40$ and Load Impedances 480 - j480 ohms

Element Number	Current Ratio	Phase Difference (degrees)
$\phi_{inc} = -40$ degrees		
1	1.001	0.23
2	1.012	0.40
3	1.015	-0.63
4	0.993	-1.32
5	0.973	0.16
6	0.998	1.34
7	1.016	0.42
8	1.020	-0.36
$\phi_{inc} = -60$ degrees		
1	1.004	0.03
2	0.997	0.59
3	1.003	0.98
4	1.013	0.92
5	1.021	0.43
6	1.023	-0.18
7	1.003	-0.65
8	1.032	-1.71

Table 1d - Comparison of Load Currents From Eq. (4) With Those From the Method of Ref. 1 for $\beta_{0h} = 1.80$ and Load Impedances 480 - j480 ohms

Element Number	Current Ratio	Phase Difference (degrees)
$\phi_{inc} = -40$ degrees		
1	0.964	0.38
2	0.982	0.07
3	0.984	0.82
4	0.996	0.77
5	0.996	0.50
6	0.992	0.68
7	0.995	1.27
8	1.004	1.38
$\phi_{inc} = -60$ degrees		
1	1.000	2.04
2	1.011	0.28
3	0.999	-1.55
4	0.986	-2.56
5	0.988	-2.33
6	1.003	-1.10
7	1.016	0.51
8	1.007	1.85

Security Classification

DOCUMENT CONTROL DATA - R & D

(Security classification of title, body of abstract and indexing annotation must be entered when the overall report is classified)

ORIGINATING ACTIVITY (Corporate author)

Naval Research Laboratory
Washington, D.C. 20390

2a. REPORT SECURITY CLASSIFICATION

UNCLASSIFIED

2b. GROUP

REPORT TITLE

DISLOCATION PIPE DIFFUSION IN SILVER SINGLE CRYSTALS

DESCRIPTIVE NOTES (Type of report and inclusive dates)

This report completes one phase of problem; work on other phases continues.

AUTHOR(S) (First name, middle initial, last name)

R. G. Vardiman and M. R. Achter

REPORT DATE

March 25, 1969

7a. TOTAL NO OF PAGES

14

7b. NO OF REFS

17

8. CONTRACT OR GRANT NO

NRL Problem M01-09

9a. ORIGINATOR'S REPORT NUMBER(S)

NRL Report 6869

b. PROJECT NO

RR 007-01-46-5407

9b. OTHER REPORT NO(S) (Any other numbers that may be assigned this report)

10. DISTRIBUTION STATEMENT

This document has been approved for public release and sale; its distribution is unlimited.

11. SUPPLEMENTARY NOTES

12. SPONSORING MILITARY ACTIVITY

Department of the Navy
(Office of Naval Research),
Washington, D.C. 20360

13. ABSTRACT

A chemical sectioning technique has been developed for the measurement of self diffusion in silver at low temperatures. (Silver was chosen because of its well-established high-temperature behavior, and because of the availability of the long-lived isotope Ag^{110} .) Layers of 100A or less are removed by an iodine reaction, and diffusion coefficients D as low as 2×10^{-17} cm²/sec have been measured. A large enhancement over extrapolated high-temperature values, which has been observed below $T_m/2$, is attributed to dislocation short circuiting. Determination of the pipe diffusion coefficient at the lowest measured temperature, where Harrison's type C kinetics are expected to apply, yields good agreement with the pipe diffusion coefficients D_p calculated from published data obtained by another technique.

14 KEY WORDS	LINK A		LINK B		LINK C	
	ROLE	WT	ROLE	WT	ROLE	WT
Diffusion coefficient Single crystals Silver Silver isotopes Crystal dislocations						